

Accumulative Magnetic Switching of Ultrahigh-Density Recording Media by Circularly Polarized Light

Y. K. Takahashi,^{1,*} R. Medapalli,² S. Kasai,¹ J. Wang,¹ K. Ishioka,¹ S. H. Wee,³
O. Hellwig,^{4,5} K. Hono,¹ and E. E. Fullerton²

¹National Institute for Materials Science,
1-2-1 Sengen, Tsukuba 305-0047, Japan

²Center for Memory and Recording Research, University of California San Diego,
9500 Gilman Drive, La Jolla, California 92093-0401, USA

³San Jose Research Center, HGST a Western Digital company, 3403 Yerba Buena Road,
San Jose, California 95135, USA

⁴Institut für Ionenstrahlphysik und Materialforschung, Helmholtz-Zentrum Dresden-Rossendorf,
Bautzner Landstrasse 400, 01328 Dresden, Germany

⁵Institut für Physik, Technische Universität Chemnitz, 09126 Chemnitz, Germany

(Received 2 May 2016; revised manuscript received 25 August 2016; published 14 November 2016)

Magnetization control of ferromagnetic materials only by circularly polarized light has received increasing attention both as a fundamental probe of the interactions of light and magnetism but also for future high-density magnetic recording technologies. Here we show that for granular FePt films designed for ultrahigh-density magnetic recording, the optical magnetic switching by circularly polarized light is an accumulative effect from multiple optical pulses. The measured results can be reproduced by a simple statistical model where the probability of switching a grain depends on the helicity of the optical pulses. We further show the deterministic switching of high-anisotropy materials by the combination of circularly polarized light and modest external magnetic fields, thus, revealing a pathway towards technological implementation.

DOI: 10.1103/PhysRevApplied.6.054004

I. INTRODUCTION

Deterministic control of magnetization by light, often referred to as all-optical switching (AOS), is an attractive recording method for magnetic nanotechnologies because magnetization control becomes possible without the need of an external magnetic field [1–5] and, therefore, incorporates the potential for ultrafast magnetization switching up to 1000 times faster than that by magnetic fields while using lower energies [6]. The first demonstration of the magnetization switching by light was in a ferrimagnetic GdFeCo film, which is a magneto-optical material [1] where the Gd and FeCo spin sublattices are antiferromagnetically exchange coupled. While several mechanisms for the ultrafast magnetization switching of GdFeCo have been explored [7–9], the current understanding for AOS in GdFeCo is that the ultrafast laser excitation demagnetizes the two sublattices at different time scales [6] resulting in a transient ferromagnetic state where the Gd and FeCo sublattices are parallel. At later times, as the Gd moment reemerges in the antiparallel orientation due to the exchange interaction, the sublattice moments end up in the opposite direction as compared to the initial state. The deterministic helicity-dependent switching observed in the experiments results from helicity-dependent absorption

(dichroism) which favors one magnetic configuration over the other for a narrow range of fluence [10].

It was believed that AOS occurs only in ferrimagnetic materials including synthetic structures [1–4] since the mechanism determined for GdFeCo films required antiparallel exchange of two sublattice systems. However, Lambert *et al.* [5] reported the deterministic optical control of magnetization in ferromagnets including Co-based multilayer thin films and FePtAg-C granular thin-film materials. Therefore, the potential mechanisms for AOS in ferromagnetic materials must be reexamined. In addition, the observation of AOS in granular FePt-based films being developed for heat-assisted magnetic recording (HAMR) [11,12] directly impacts the magnetic recording community, since it provides a potential solution to the so-called “trilemma problem” in high-density hard disk drives beyond 1 Tbit/in² [2,13,14]. Here, to probe both the mechanisms of optical reversal and its potential for technological applications, we report the observation of accumulative magnetic switching from multiple circularly polarized light pulses on FePt-C granular HAMR media.

II. EXPERIMENT

The FePt-30vol %C (hereafter, FePt-C) granular film is deposited by cosputtering of FePt and C targets on a MgO(001) single-crystal substrate by dc magnetron sputtering under 0.48-Pa Ar pressure at 600 °C. After the

*Corresponding author.
takahashi.yukiko@nims.go.jp

deposition of 10-nm-thick FePt-C, the sample is cooled down to RT and 10-nm-thick C is deposited as a capping layer. In this work, we use a compositionally graded sputtering method to obtain the columnar FePt grains [15]. In this process, the C composition gradually changes during the deposition, which gives the nice FePt grain isolation shown in Fig. 2(a). To investigate the morphological effect on AOS, a 10-nm-thick FePt continuous film is prepared by the sputtering from an FePt alloy target under 0.48-Pa Ar pressure at 400°C. A 10-nm-thick C capping is deposited on the FePt continuous film at RT. We further study composite FePt-C/FePt structure where the FePt-C granular layer is deposited at 600°C as described above and then an FePt layer is deposited at 400°C, and, therefore, the degree of $L1_0$ ordering is lower than that of the FePt-C granular layer. The detailed description of the film processing conditions and their magnetic characteristics are reported elsewhere [16].

Hall-cross structures are used for the measurement of the magnetization change by the light exposure and/or applied magnetic fields. The Hall resistance corresponds to the average out-of-plane component in the magnetization of the FePt grains within the Hall-cross area via the anomalous Hall effect (AHE). The Hall crosses are fabricated directly from the films by photolithography using a lift-off process and a subsequent Ar ion-milling step. The width of the Hall cross is about 20 μm . The sample microstructure and magnetic properties are measured by transmission electron microscopy (TEM) and vibrating sample magnetometer, respectively. The room-temperature magnetic hysteresis of the Hall-cross area is determined by measuring the Hall resistance as a function of applied field. This measurement further allows us to normalize the Hall resistance value in optical experiments.

Figure 1 shows the optical setup for this experiment. A light-emitting diode (LED) with 590-nm wavelength is

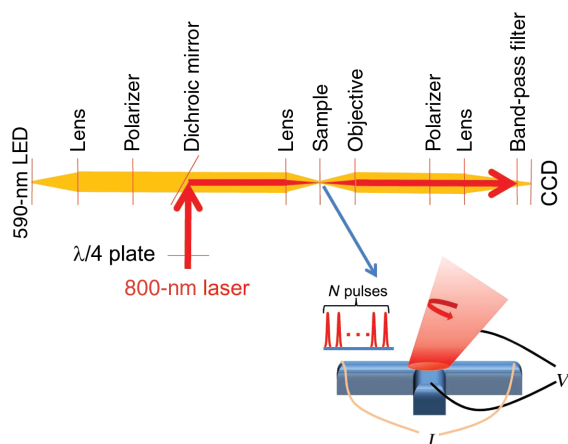


FIG. 1. Schematic of the magnetization-sensitive optical microscope combined with the Hall-cross measurement technique. The laser-induced magnetization change is obtained by measuring the corresponding change in Hall voltage across the Hall-cross arm via the anomalous Hall effect.

used for the observation of the magnetic domains of the sample in a Faraday microscope. An output of a regenerative amplifier with center wavelength of 800 nm, pulse duration of approximately 150 fs, and a repetition rate of 1 kHz is used to excite the magnetization state of the sample. The excitation pulses are focused into a spot of 30–50 μm diameter on the sample, which covers the whole region of the Hall cross. Two experiments are performed. In the first, the laser spot is slowly swept over the films or Hall crosses as done in Lambert *et al.* [5], and the optical images or Hall voltage are subsequently measured to quantify the magnetization change. In the second experiment, the laser spot is fixed to the Hall-cross area. After exposing the sample to several optical pulses, the Hall voltage is measured, and this process is repeated. The number of pulses exposed on the sample is controlled by a mechanical shutter. We estimate the laser-induced change in the magnetization from the differences in Hall resistance before and after the exposure. We apply this method to obtain the results discussed throughout this paper.

III. RESULTS

A. Microstructure and magnetic properties of FePt continuous and granular films

Figure 2(a) shows a plan-view TEM bright-field image of the FePt-C films along with the corresponding nanobeam diffraction (ND) pattern and histogram of the grain

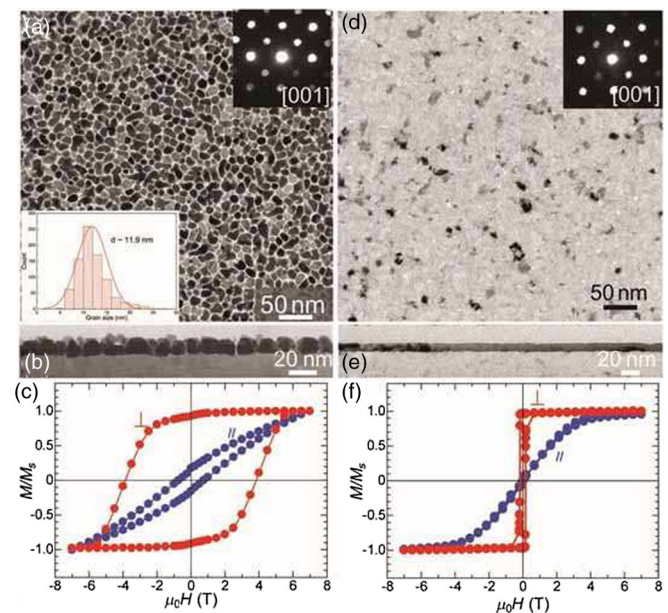


FIG. 2. Microstructure and magnetic properties of FePt-C and FePt films. (a) Plan-view TEM bright field image. The corresponding nanobeam diffraction pattern and histogram of FePt grain size are shown in the insets, (b) a cross-sectional TEM image, and (c) magnetization curves of the FePt-C granular film. (d),(e),(f) are the same as (a),(b),(c), respectively, but for the corresponding FePt continuous film.

sizes. The dark contrast areas are the FePt grains and the bright contrast area is the carbon (C) segregant. The average grain size is approximately 11.9 nm, and these grains are distributed within an amorphous C matrix. The ND pattern indicates that all of the FePt grains have strong (001) texture because of the epitaxial growth on the MgO(001) single-crystal substrate. Figure 2(b) shows a cross-sectional TEM image of the FePt-C granular film. The aspect ratio of the FePt grains is roughly 1. Figure 2(c) shows the magnetization curves of the FePt-C granular film. The red and blue symbols correspond to the magnetization with the applied magnetic field perpendicular and parallel to the film surface, respectively. The film shows strong perpendicular magnetic anisotropy with a saturation field of 7 T for the in-plane applied field and high coercive field ($\mu_0 H_c$) of 4 T when the field is applied normal to the surface due to the strong (001) texture and highly $L1_0$ -ordered FePt grains.

Figure 2(d) shows the plan-view TEM bright field image and ND pattern of the FePt continuous film. The film shows a continuous microstructure and epitaxial growth on the MgO(001) substrate. In contrast to the magnetic properties of the granular film shown in Fig. 2(c), the $\mu_0 H_c$ of the FePt continuous film is only 0.17 T due to the small number of pinning sites for domain-wall motion. Although the $\mu_0 H_c$ is small, the anisotropy field is about 4 T. The smaller anisotropy field in FePt continuous films is attributed to the low degree of $L1_0$ ordering ($S = 0.51$) caused by lower deposition temperature of 400 °C.

B. AOS in FePt-C granular media

Figures 3(a) and 3(b) show the magneto-optical images at remanence of an initially demagnetized sample [Fig. 3(a)] and a sample after saturation at 7 T [Fig. 3(b)] for FePt-C granular film after scanning it with both right-circularly-polarized (RCP) and left-circularly-polarized (LCP) light pulses. The fluence of the laser is 35.7 mJ/cm² and 48.1 mJ/cm² for Figs. 3(a) and 3(b), respectively. As is reported in Ref. [5], the optical pulses induce a net magnetization in the FePt granular media, and the sign of the magnetization is determined by the helicity of the light. To quantify the optically induced magnetization, Hall resistance changes are normalized by the field-dependent hysteresis loop, which reveals approximately 2.75- Ω change in Hall resistance between negative and positive saturation in Fig. 3(c). We first sweep the laser over the Hall cross in a similar way as shown in Fig. 3(a) and measure an induced magnetization. It is roughly 66% of the saturation magnetization as shown in Fig. 3(c). The fluence of the laser is 35.7 mJ/cm². We then fix the laser over the Hall-cross region to measure the evolution of the magnetization to a series of ultrafast laser pulses. We initially use 40 optical pulses of 101.9 mJ/cm² for the first three exposures and then increase to 80 pulses for the next five to six exposures. In Figs. 3(d) and 3(e), the dashed line shows the

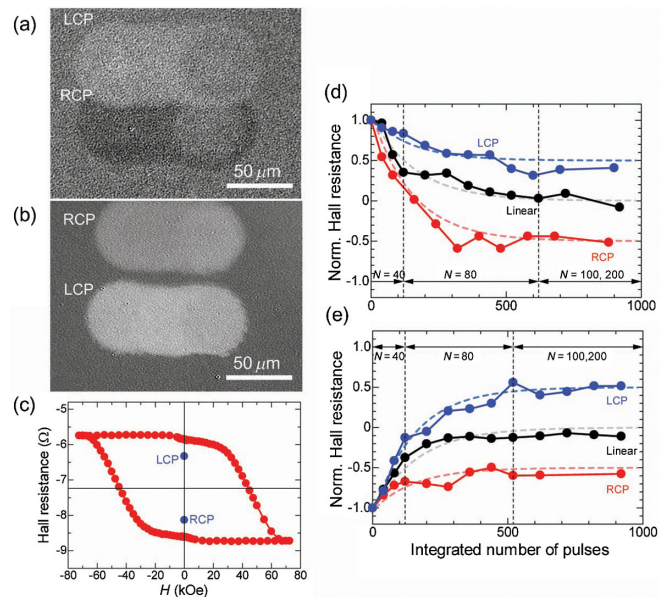


FIG. 3. Magnetization change observed from an FePt-C granular film by exposure to circularly polarized light. (a) Magneto-optical image after slow sweeping of the LCP and RCP pulsed laser beam at a repetition rate of 1 kHz. The fluence is 35.7 mJ/cm². The sample is initially demagnetized. Note that we show a subtracted image obtained from before and after applying the laser exposure. (b) same as (a), but the sample is initially in the remanent state after applying a magnetic field of 7 T. The fluence is 48.1 mJ/cm². (c) AHE curve for the FePt-C granular film. The additional data points at zero field correspond to the amount of magnetization switched by sweeping right and left circularly polarized light in the Hall cross in a similar way as shown in (a) and (b). (d) Normalized Hall resistance after applying circularly and linearly polarized light as a function of the integrated number of pulses. Red, blue, and black dots correspond to the normalized Hall resistance after applying RCP, LCP, and linearly polarized light. The initial state is the spin-up state in all FePt grains. The dotted lines show the fit obtained using the accumulative magnetic switching model described in the main text. The fluence is 101.9 mJ/cm². (e) Normalized Hall resistance after illumination with RCP, LCP, and linearly polarized light. The initial state is the spin-down state in all FePt grains.

change of the number of pulses for each exposure. The Hall resistance is measured after each sequence and then plotted as a function of the integrated number of pulses. The initial state is remanence after applying saturating magnetic fields of -7 T [Fig. 3(d)] and 7 T [Fig. 3(e)]. Figure 3(d) shows the normalized Hall resistance change after the exposure to RCP, linearly polarized, and LCP optical pulses. For RCP light, the normalized magnetization gradually decreases to zero then reverses and saturates at about -0.5 . This indicates that approximately 3/4 of the FePt grains switch to the opposite direction. On the other hand, the exposure to LCP light decreases the magnetization to about half of the initial value, corresponding to the switching of approximately 1/4 of the FePt grains. For exposure to linearly

polarized light, the normalized Hall resistance gradually approaches zero, indicating that half of the grains switch. In the case of the opposite initial state (negative saturation) shown in Fig. 3(e), RCP, LCP, and linearly polarized light exposures result in the same final normalized magnetization of -0.5 , 0.5 , and zero, respectively. The results suggest that the magnetization state after exposure to polarized light depends only on the helicity of the light and is independent of the initial magnetization state. More important, the results show that the final state is reached only after approximately 500 pulses are applied for this specific laser power.

Figure 4 shows the change of the normalized Hall resistance in an FePt-C film measured with increasing pulse number. The sample is exposed between measurements at the laser powers of 79.6 mJ/cm^2 for Fig. 4(a) and 107.5 mJ/cm^2 for Fig. 4(b). The initial state is spin-up for all FePt grains, and the sample is exposed to RCP light. At the lower power of 79.6 mJ/cm^2 shown in Fig. 4(a), exposing the sample to a series of 20 optical pulses does not significantly perturb the system. By increasing the number of pulses between measurements of the Hall voltage, the magnetization decreases. However, we do not observe a net switching into the opposite direction. This indicates that the small laser power does not provide

sufficient instantaneous heat for a significant magnetization switching to occur but that only accumulated heat from many optical pulses at 1-kHz repetition rate can slowly thermally demagnetize the sample. At higher power of 107.5 mJ/cm^2 shown in Fig. 4(b), the Hall resistance decreases much faster after the first laser exposure. In sets of 20 and 40 pulses, the Hall resistance decreases significantly by illumination of RCP light; however, the overall magnetization direction of the film still remains positive, just as for the initial state. When using sets of 60 and 80 pulses, the normalized Hall resistance then changes sign to -0.5 . However, for sets of 160 pulses at a time, the normalized Hall resistance decreases only to -0.4 , which may be due to excess accumulated heat in the sample from the longer sequence of pulses. Further increase of the pulse number, such as 1000 pulses, results in a non-monotonous and nonreproducible behavior after the exposure of 10 000 pulses (ten sequences), and the AHE versus magnetic field curve is no longer the same as that before the laser exposure. This means that the Hall cross received destructive damage by the 1000-pulse sequence. Independent of laser conditions, the maximum optically induced magnetization switching using a fixed laser beam is roughly half the saturation magnetization and is an accumulative effect using multiple optical pulses.

C. Morphological effect on AOS

To probe the microstructural effect on the magnetization switching, we compare the Hall resistance change between granular FePt-C and a continuous 10-nm-thick FePt film. Figure 5 shows the normalized Hall resistance change as a function of the fluence of RCP optical pulses in FePt-C granular and FePt continuous films. The normalized Hall resistance decreases in both of the samples. However, in contrast to the granular FePt film, the continuous film simply demagnetizes with further increase of the RCP light

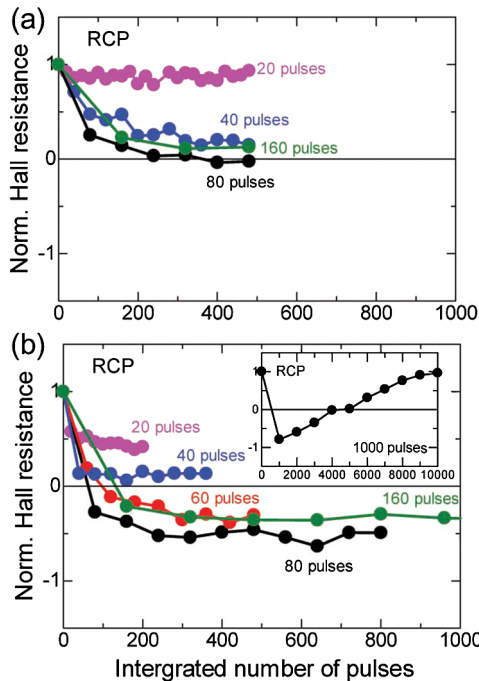


FIG. 4. Normalized Hall resistance that corresponds to the net magnetization in the film is plotted against the sequence of pulses used to pump. (a) shows the curves for various sequences of the number of RCP pulses varying from 20 to 160 pulses with a fluence of 79.6 mJ/cm^2 . (b) is the same as (a) but for a fluence of 107.5 mJ/cm^2 . The inset shows the same as (b) for the sequence of 1000 pulses.

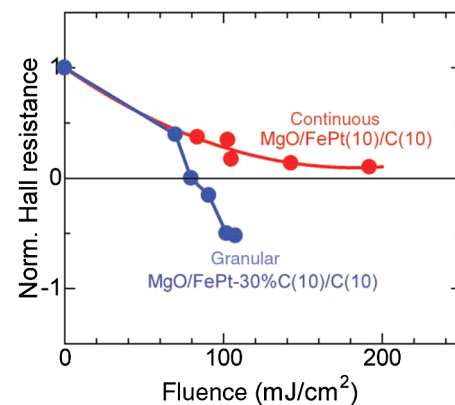


FIG. 5. Normalized Hall resistance for FePt continuous (red) and FePt-C granular (blue) films versus fluence. The initial state is spin-up in FePt grains. The number of pulses is 80 for both samples. RCP light is used.

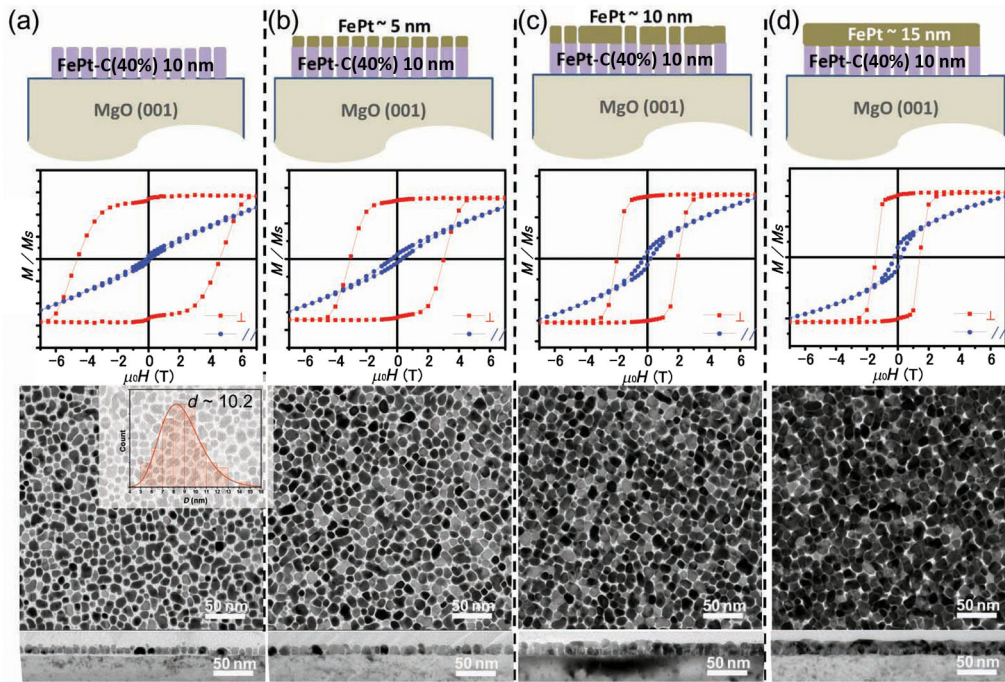


FIG. 6. (Top) Schematic of the film, (center) magnetization curves, and (bottom) microstructure of FePt-C ECC media are shown for various thicknesses of the semihard FePt layer of (a) 0 nm, (b) 5 nm, (c) 10 nm, and (d) 15 nm [5].

pulse fluence, which is consistent with the thermal demagnetization and the formation of domains as seen in thick Co/Pt multilayer films [5] driven by strong dipolar energies. In the granular film, the dipole energy is much smaller than that of the continuous film, and the magnetization reversal cannot progress by domain-wall motion because of the break in magnetic exchange between the magnetic grains. When the fluence is higher than 107.5 mJ/cm^2 , the FePt-C granular films receive destructive damage because of the poor thermal conductivity. We further observe a continuous transitional behavior between these two extreme behaviors in intermediate exchange composite granular or continuous films, as we show in the next section.

D. AOS in exchange-coupled composite media

Exchange-coupled composite (ECC) media are proposed in order to ameliorate the so-called “trilemma problem” in magnetic recording [13,14,17]. By putting the magnetically soft layer on top of the CoCrPt or FePt granular layer, the switching field can be effectively reduced while maintaining the energy barrier for the magnetization rotation [13,14,18,19]. Wang *et al.* [16] report a significant reduction of switching field in FePt-C granular media by adding a continuous FePt layer to the high-anisotropy granular layer, which we use for the AOS experiment here. Figure 6 shows the schematic view of the film stack, magnetization curves, and microstructures of the ECC media with various FePt layer thicknesses. With increasing the FePt layer thickness from 0 to 15 nm, the morphology of the capping layer is changed from partially granular to continuous, and the perpendicular $\mu_0 H_c$ reduces from 4.9 to 1.4 T.

Figure 7 shows the change of the normalized Hall resistance of the initially demagnetized films after exposure to RCP light across the Hall cross at a fluence of 24.5 mJ/cm^2 . The magnetization switching ratio decreases with increasing thickness of the FePt layer. The inset shows the Hall resistance changes by circular polarized light in FePt-C/FePt(15 nm) ECC media. The magnetization switches depending on the helicity of the light and shows zero when linearly polarized light is used. The resistance change by the light illumination is reproducible. However, the magnetization switching ratio is very small, only 1.5%. These results also support that the large dipole energy and

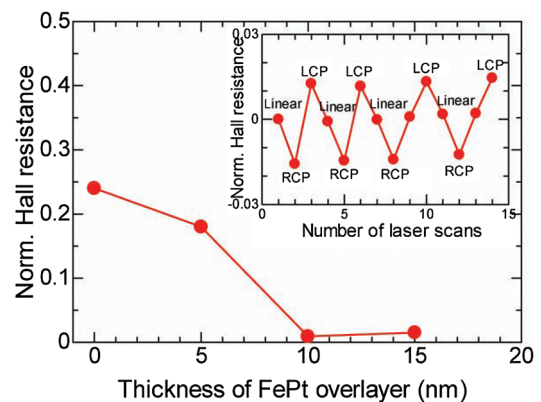


FIG. 7. Normalized Hall resistance measured after the laser-beam exposure in the FePt-C ECC media are plotted as a function of the thickness of the FePt semihard layer. The laser fluence is 24.5 mJ/cm^2 . The inset shows how the normalized Hall resistance toggles between the negative and positive values via zero when the exposed laser-beam helicity is changed from left circular via linear to right circular polarization back and forth.

domain formation allow only for a small magnetization switching in the continuous film.

E. Deterministic switching in FePt-C granular media

To achieve deterministic switching, we additionally apply a small external magnetic field, while applying 80 optical pulses at a fluence of 107.5 mJ/cm^2 for each sequence. Figure 8(a) shows the normalized Hall resistance change after the exposure to linearly polarized laser under an external magnetic field of 0.051 T . Regardless of the polarity of the external magnetic field, the magnetization of the FePt-C granular film remains close to the demagnetized state. When the external magnetic field is increased to approximately 0.2 T as shown in Fig. 8(b), the magnetization changes depend on the external magnetic field polarity, but only about half of the total magnetization can be switched by a 0.2-T field. This result is consistent with earlier studies observing the combined effect of optical pulse and applied magnetic fields in FePt media where a 0.5-T field is required to saturate the magnetization [20]. In the HAMR process, the applied magnetic field is not needed to overcome the coercive field but overcome thermal activation of the nanoparticles near T_C . However, by the combination of the circularly polarized light and an external magnetic field of 0.2 T , a magnetization reversal $>90\%$ of the saturation

magnetization can be achieved as shown in Fig. 8(c), and, thus, the use of circularly polarized light greatly lowers the applied field and increases the effective magnetic field gradient for HAMR.

IV. DISCUSSION

To understand the switching mechanism by circularly polarized light in FePt granular film, the data shown in Figs. 3(d) and 3(e) are fitted by a simple accumulative switching model where we treat the FePt grains as having two magnetic states, spin-up and spin-down states, because of its high magnetic anisotropy and small grain size. The total number of FePt grains N is expressed by the summation of spin-up grains N_\uparrow and spin-down grains N_\downarrow , and the normalized magnetization is given by $(N_\uparrow - N_\downarrow)/(N_\uparrow + N_\downarrow)$. We assume that with each optical pulse there is a switching probability from the spin-up to spin-down state given by P_1 and from the spin-down to spin-up state by P_2 . The number of FePt grains with spin-up and spin-down states after the n th pulse can be expressed by the state after the $(n - 1)$ pulse following

$$N_\uparrow^n = N_\uparrow^{n-1}(1 - P_1) + N_\downarrow^{n-1}P_2 \quad \text{and} \quad N_\downarrow^n = N - N_\uparrow^n. \quad (1)$$

The fitted lines to Eq. (1) are shown in Figs. 3(d) and 3(e) using the same switching probabilities for RCP, LCP, and linearly polarized light exposure: $(P_1, P_2) = (0.0048, 0.0016)$, $(0.0016, 0.0048)$, and $(0.0032, 0.0032)$, respectively. The calculations assume $N_\uparrow^{n=0} = N$ for Fig. 3(d) and $N_\uparrow^{n=0} = 0$ for Fig. 3(e). The fits describe the data well and suggest that the switching probability by a single pulse is very small, less than 1%. However, accumulating the small switching probabilities results in a continuous change in the magnetization until the final equilibrium state where $N_\uparrow P_1 = N_\downarrow P_2$ [a final-state normalized magnetization of $(P_2 - P_1)/(P_2 + P_1)$] is reached. This final state is independent of the initial state of the magnetization, as seen experimentally. The switching probability for the linearly polarized light is given by approximately $(P_1 + P_2)/2$ because the linearly polarized light is composed of a combination of equal amount of LCP and RCP light. The switching probability P could be a function of the total magnetization, temperature, and specific heat as suggested by the results in Fig. 4. However, to keep the discussion part simple, we assume that the P_1 and P_2 remain the same, or they change by a small amount after every next pump pulse excitation.

What is the origin for different switching probability of P_1 and P_2 for circularly polarized light pulses? The fact that linear light leads to demagnetization of the sample suggests that heating of the FePt grains by the femtosecond laser exposure is sufficient to cause thermally activated reversal. The circularly polarized light then breaks the symmetry of the system favoring one magnetic state over the other and

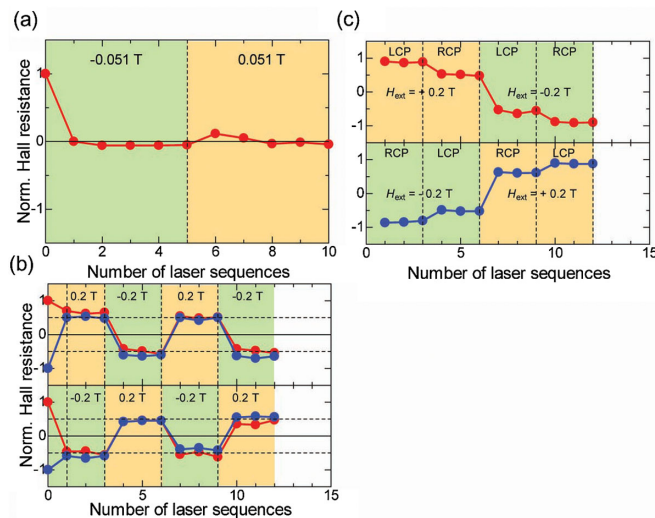


FIG. 8. (a) Normalized Hall resistance is plotted as a function of the number of sequences N , for the case of linearly polarized light under the influence of an external magnetic field of $\pm 0.051 \text{ T}$. Note the change of magnetic field direction after the exposure of $N = 5$. (b) is the same as (a) but with a higher external magnetic field of $\pm 0.2 \text{ T}$. The blue curve shows the data for the case when the initial magnetic state is along the spin-down direction and the red one for the spin-up direction. The pulse number in each sequence is 80. The light fluence is 107.5 mJ/cm^2 . (c) is the same as (b) but for the cases of left and right circularly polarized light sequences. The data are shown for both cases, with the initial magnetization state along the spin-up (red) and spin-down (blue) direction.

leading to an imbalance in P_1 and P_2 . This symmetry breaking could result from a direct interaction between the light and the magnetic systems such as the inverse Faraday field that prefers one direction over the other [21]. The difference in P_1 and P_2 could also arise from differential absorption for RCP and LCP (i.e., magnetic circular dichroism) that will result in a slight difference in temperature for one set of grains compared to the other [10]. We roughly estimate the difference in the temperature needed during the optical excitation to explain the difference in the switching probability using a simple Arrhenius-Néel model for single-domain particles where the time dependence of magnetization of an ensemble of particles versus time (t) is given by

$$M(t) = M(t=0) \exp\left(\frac{-t}{\tau}\right), \quad (2)$$

where τ is the characteristic time for thermal switching. In zero external field, τ is given by

$$\tau = \tau_0 \exp\left(\frac{K_u V}{k_B T}\right), \quad (3)$$

where $K_u V$ is the magnetic energy of the particle that is the product of the magnetic anisotropy K_u , and the particle volume V and τ_0 is the attempt time for thermal activation (typically 0.1 ns for high-anisotropy magnetic systems). Assuming that $M(t)/M(t=0)$ equals $1 - P_1$ for RCP light and $1 - P_2$ for LCP, then one can estimate $\tau_{\text{LCP}}/\tau_{\text{RCP}}$ assuming the time t is the same for RCP and LCP excitation by

$$\frac{\tau_{\text{LCP}}}{\tau_{\text{RCP}}} = \frac{\ln(1 - P_1)}{\ln(1 - P_2)}. \quad (4)$$

Combing Eqs. (2) and (3), we can estimate the difference in $K_u V/k_B T$ between RCP and LCP excitations, which is given by

$$\left(\frac{K_u V}{k_B T}\right)_{\text{LCP}} - \left(\frac{K_u V}{k_B T}\right)_{\text{RCP}} = \ln\left(\frac{\tau_{\text{LCP}}}{\tau_{\text{RCP}}}\right). \quad (5)$$

For $P_1 = 0.0048$ and $P_2 = 0.0016$, Eq. (4) gives $\tau_{\text{LCP}}/\tau_{\text{RCP}} = 3.005$, and the corresponding difference in $K_u V/k_B T$ between the LCP and RCP excitations from Eq. (5) is 1.1.

From the properties of FePt grains, we estimate the temperature difference to result in a change in $K_u V/k_B T$ of 1.1. For a magnetic grain with 12 nm diameter, 10 nm height, and a magnetic anisotropy of $K_u = 4.3 \times 10^7$ ergs/cm³, we can estimate that room temperature $K_u V/k_B T$ is approximately 1200. Since $K_u V/k_B T$ goes to zero at $T_C \sim 700$ K, we can roughly estimate that $K_u V/k_B T$ decreases on the order of 3 per K temperature change. This estimation suggests that there is only a small difference in the temperature of approximately 1/3 K due to excitation of RCP and LCP that is consistent with the

observed P_1 and P_2 values and with typical dichroism differences in magnetic metals [10]. However, these estimates ignore any interactions between grains, any distributions in grain size, or the specific dependence of the temperature on time after excitation. Since the submission of this article, three recent papers have modeled the thermal origin difference in P_1 and P_2 in significant detail and qualitatively agree with the arguments given above [22–24].

We can further estimate how close to T_C we have to heat the sample to observe the statistical switching that we find. Using Eqs. (1) and (2) and assuming that the sample is heated for 1 ns, $K_u V/k_B T$ needs to be 7.6 for $P_1 = 0.0048$ and 8.7 for $P_2 = 0.0016$, suggesting that we are heating close to T_C . This observation can also explain, in part, the results in Fig. 4 where the demagnetization and optical reversal depend on the number of consecutive pulses. While one may think that with a repetition rate of 1 kHz that there is sufficient time to cool down to ambient temperature between pulses, there appears to be some accumulated heating. However, heating of only 1 K is sufficient to change the switching probabilities since we are heating close to T_C . In the case of the FePt continuous film, the absorbed heat from the light can be dispersed quickly. Therefore, the film is not irreversibly damaged even at 190 mJ/cm². However, for the granular film, FePt grains are heated more effectively by the light exposure because of the thermal isolation of adjacent grains by the amorphous carbon segregant whose thermal conductivity is more than 10 times lower than that of FePt. Laser exposure higher than 120 mJ/cm² results in irreversible damage of the FePt-C granular film.

Since we do not have experimental results on how the inverse Faraday field affects the switching process, we cannot conclude whether the AOS process is governed by only magnetic circular dichroism (MCD). Note that John *et al.* [25] investigated experimentally and theoretically the AOS of FePt-C media. They reported that the magnetization switching in FePt grains is a stochastic process and multiple pulses are necessary to switch, which agrees with our results. Based on modeling, they concluded that the deterministic switching will be possible with both MCD and inverse Faraday effect (IFE). Ellis *et al.* [22] concluded from modeling that IFE alone without MCD requires very high IFE fields, and experimental results can be understood solely from MCD.

Here, we show the deterministic magnetization switching of the combination of circularly polarized light and modest external magnetic fields compared to HAMR. In currently developed so-called “small-thermal-spot HAMR,” the thermal spot is much smaller than the magnetic field spot. The magnetic field spot has a dimension of microns, while the heat spot is only a few tens of nanometers in diameter. Therefore, the bit transitions and the track width are defined by the thermal spot. If circularly

polarized light can be used as the thermal spot, it acts on the same length scale as the thermal spot of current near-field transducers (NFTs) but required NFTs to produce circularly polarized light [26]. In addition, the smaller magnetic field which is necessary for complete write may allow us to push the writing point closer to the Curie point, which means generally a steeper anisotropy field (H_K) versus temperature slope. Both of these effects should then increase the effective magnetic field gradient when writing the transitions and also sharpen the track edge profile, allowing smaller tracks and sharper bit transitions since part of the magnetic reversal is now triggered by the small thermal spot, and the writing point may be pushed closer towards T_c . Therefore, we can expect that the circularly polarized light can aid the writing in a HAMR-like recording process and lowers the external field required which is important for scaling of HAMR to higher areal densities.

V. CONCLUSION

In conclusion, we show that the optical magnetic switching for granular FePt films designed for ultrahigh-density recording by circularly polarized light is an accumulative effect of multiple optical pulses. This is qualitatively different from the AOS mechanism for GdFeCo but closer to the behavior reported for Pt/Co/Pt structures [26]. The observed AOS in FePt granular media can be described by a statistical model considering a small probability of switching magnetic grains for each light pulse, and these probabilities depend on the helicity of the light. It results in a high degree of alignment of FePt grains of approximately 75% achieved only with multiple circularly polarized optical pulses. We further show that deterministic magnetization switching is achievable by the combination of circularly polarized light and modest external magnetic fields demonstrating that the circularly polarized light can aid the writing in a HAMR-like recording process. This study also suggests that the fully deterministic switching using only AOS for high-anisotropy nanostructures may require more complex structures or application and control of an optically induced magnetic field.

ACKNOWLEDGMENTS

This work is supported in part by Grand-in-Aid for Scientific Research (B) Grant No. 26289232, and the work at University of California San Diego is supported by the Office of Naval Research MURI program.

-
- [1] C. D. Stanciu, F. Hansteen, A. V. Kimel, A. Kirilyuk, A. Tsukamoto, A. Itoh, and Th. Rasing, All-Optical Magnetic Recording with Circularly Polarized Light, *Phys. Rev. Lett.* **99**, 047601 (2007).
 [2] A. Hassdenteufel, B. Hebler, C. Schubert, A. Liebig, M. Teich, M. Helm, M. Aeschlimann, M. Albrecht, and

- R. Bratschitsch, Thermally assisted all-optical helicity dependent magnetic switching in amorphous $\text{Fe}_{100-x}\text{Tb}_x$ alloy films, *Adv. Mater.* **25**, 3122 (2013).
 [3] S. Alebrand, M. Gottwald, M. Hehn, D. Steil, M. Cinchetti, S. Lacour, E. E. Fullerton, M. Aeschlimann, and S. Mangin, Light-induced magnetization reversal of high-anisotropy TbCo alloy films, *Appl. Phys. Lett.* **101**, 162408 (2012).
 [4] S. Mangin, M. Gottwald, C.-H. Lambert, D. Steil, V. Uhlir, L. Pang, M. Hehn, S. Alebrand, M. Cinchetti, G. Malinowski, Y. Fainman, M. Aeschlimann, and E. E. Fullerton, Engineered materials for all-optical helicity-dependent magnetic switching, *Nat. Mater.* **13**, 286 (2014).
 [5] C.-H. Lambert, S. Mangin, B. S. D. Ch. S. Varaprasad, Y. K. Takahashi, M. Hehn, M. Cinchetti, G. Malinowski, K. Hono, Y. Fainman, M. Aeschlimann, and E. E. Fullerton, All-optical control of ferromagnetic thin films and nanostructures, *Science* **345**, 1337 (2014).
 [6] I. Radu, K. Vahaplar, C. Stamm, T. Kachel, N. Pontius, H. A. Dürr, T. A. Ostler, J. Barker, R. F. L. Evans, R. W. Chantrell, A. Tsukamoto, A. Itoh, A. Kirilyuk, Th. Rasing, and A. V. Kimel, Transient ferromagnetic-like state mediating ultrafast reversal of antiferromagnetically coupled spins, *Nature (London)* **472**, 205 (2011).
 [7] A. Kirilyuk, A. V. Kimel, and T. Rasing, Ultrafast optical manipulation of magnetic order, *Rev. Mod. Phys.* **82**, 2731 (2010).
 [8] G. P. Zhang and W. Hubner, Laser-Induced Ultrafast Demagnetization in Ferromagnetic Metals, *Phys. Rev. Lett.* **85**, 3025 (2000).
 [9] C. E. Graves *et al.* Nanoscale spin reversal by non-local angular momentum transfer following ultrafast laser excitation in ferrimagnetic GdFeCo, *Nat. Mater.* **12**, 293 (2013).
 [10] A. R. Khorsand, M. Savoini, A. Kirilyuk, A. V. Kimel, A. Tsukamoto, A. Itoh, and Th. Rasing, Role of Magnetic Circular Dichroism in All-Optical Magnetic Recording, *Phys. Rev. Lett.* **108**, 127205 (2012).
 [11] M. H. Kryder, E. C. Gage, T. W. McDaniel, W. A. Challener, R. E. Rottmayer, G. P. Ju, Y. T. Hsia, and M. F. Erden, Heat assisted magnetic recording, *Proc. IEEE* **96**, 1810 (2008).
 [12] B. C. Stipe, T. C. Strand, C. C. Poon, H. Balamane, T. D. Boone, J. A. Katine, J. Li, V. Rawat, H. Nemoto, A. Hirotsune, O. Hellwig, R. Ruiz, E. Dobisz, D. S. Kercher, N. Robertson, T. R. Albrecht, and B. D. Terris, Magnetic recording at 1.5 Pb m^{-2} using an integrated plasmonic antenna, *Nat. Photonics* **4**, 484 (2010).
 [13] D. Suess, T. Schrefl, S. Faehler, M. Kirschner, G. Hrkac, F. Dorfbauer, and J. Fidler, Exchange spring media for perpendicular recording, *Appl. Phys. Lett.* **87**, 012504 (2005).
 [14] R. H. Victora and X. Shen, Composite media for perpendicular magnetic recording, *IEEE Trans. Magn.* **41**, 537 (2005).
 [15] B. S. D. Ch. S. Varaprasad, J. Wang, T. Shiroyama, Y. K. Takahashi, and K. Hono, Columnar structure in FePt-C granular media for heat-assisted magnetic recording, *IEEE Trans. Magn.* **51**, 3200904 (2015).
 [16] J. Wang, H. Sepehri-Amin, Y. K. Takahashi, S. Okamoto, S. Kasai, J. Y. Kim, T. Schrefl, and K. Hono, Magnetization reversal of FePt based exchange coupled composite media, *Acta Mater.* **111**, 47 (2016).

- [17] E. E. Fullerton, H. V. Do, D. T. Margulies, and N. Supper, Incoherently-reversing magnetic laminate with exchange coupled ferromagnetic layers, U.S. Patent No. 7,425,377 (16 September 2008).
- [18] S. Sonobe, K. K. Tham, T. Umezawa, T. Takasu, J. A. Dumaya, and P. Y. Leo, Effect of continuous layer in CGC perpendicular recording media, *J. Magn. Magn. Mater.* **303**, 292 (2006).
- [19] D. Suess, T. Schrefl, R. Dittrich, M. Kirschner, F. Dorfbauer, G. Hrkac, and J. Fidler, Exchange spring recording media for areal densities up to 10 Tbit/in², *J. Magn. Magn. Mater.* **290–291**, 551 (2005).
- [20] S. Pisana, S. Jain, J. W. Reiner, G. J. Parker, C. C. Poon, O. Hellwig, and B. C. Stipe, Measurement of the Curie temperature distribution in FePt granular magnetic media, *Appl. Phys. Lett.* **104**, 162407 (2014).
- [21] P. Nieves and O. Chubykalo-Fesenko, Modeling of Ultrafast Heat- and Field-Assisted Magnetization Dynamics in FePt, *Phys. Rev. Applied* **5**, 014006 (2016).
- [22] M. O. A. Ellis, E. E. Fullerton, and R. W. Chantrell All-optical switching in granular ferromagnets caused by magnetic circular dichroism, *Sci. Rep.* **6**, 30522 (2016).
- [23] J. Gorchon, Y. Yang, and J. Bokor, Model for multishot all-thermal all-optical switching in ferromagnets, *Phys. Rev. B* **94**, 020409 (2016).
- [24] M. S. El Hadri, P. Pirro, C.-H. Lambert, S. Petit-Watelot, Y. Quessab, M. Hehn, F. Montaigne, G. Malinowski, and S. Mangin, Two types of all-optical magnetization switching mechanisms using femtosecond laser pulses, *Phys. Rev. B* **94**, 064412 (2016).
- [25] R. John, M. Berritta, D. Hinzke, C. Müller, T. Santos, H. Ulrichs, P. Nieves, J. Walowski, R. Mondal, O. Chubykalo-Fesenko, J. McCord, P. M. Oppeneer, U. Nowak, and M. Münzenberg, Magnetization switching of FePt nanoparticle recording medium by femtosecond laser pulses, arXiv: 1606.08723.
- [26] B. C. Stipe, All-optical magnetic recording system using circularly polarized light and bit-patterned media, U.S. Patent No. 8,164,988 B2 (24 April 2012).